

pubs.acs.org/ac Article

# Detecting Methamphetamine in Aerosols by Electroanalysis in a Soap Bubble Wall

Kathryn J. Vannoy, Nicole E. Tarolla, Philip J. Kauffmann, Rebecca B. Clark, and Jeffrey E. Dick\*



Cite This: Anal. Chem. 2022, 94, 6311-6317



**ACCESS** I

Metrics & More

Article Recommendations

SI Supporting Information

**ABSTRACT:** We present a facile method to detect methamphetamine in aerosols by trapping aerosols in a soap bubble wall for electroanalysis. A microwire was placed through a soap bubble wall as a sensing electrode along with a 1 mm diameter platinum wire as the counter/reference electrode. The resulting electrochemical cell and electrode geometry are unique and allow for reproducible electrochemistry between bubble walls. We first provide a thorough investigation of the cell and electrode geometry and an electrochemical characterization of ferrocene methanol in a soap bubble wall composed of 0.1 M KCl and 0.1% Triton X-100 (v/v). To visualize the boundary where the bubble wets the microwire (the effective electrode area) with tens of nanometer resolution, we



electrodeposited platinum on carbon microwire. Scanning electron microscopy and energy dispersive X-ray spectroscopy revealed the bubble contact (i.e., cylindrical electrode height) is  $157 \pm 30~\mu m$ . Correlated digital microscopy suggests that the wetting reaches  $r \sim 125~\mu m$  along the bubble wall laterally from the microwire. Beyond the wetting region, the bubble thickness is  $18 \pm 1~\mu m$ , as indicated by ultraviolet—visible spectroscopy experiments probing dissolved bis(bipyridine)ruthenium(II) chloride. We illustrate that the voltammetric character in this system is highly dependent on the bubble wetting parameters, which are tuned by changing the microwire material. We then applied this system to the collection and electrochemical detection of methamphetamine in liquid aerosols, where the bubble wall acts as a low volume collector.

# **■ INTRODUCTION**

Aerosol detection can be an effective means of sampling a local environment either remotely or by wearable sensors. Liquid aerosols, or small micrometer droplets suspended in air, can be useful for real-time detection of environmental pollutants, explosive materials, and illicit substances. Vapors of these aerosols can be quickly sensed without purposeful sampling or can be purposefully collected from breath to report on various toxins, viruses, or drugs. Methamphetamine is a commonly abused substance and is often smoked in a pipe releasing aerosols. Low cost, highly pure methamphetamine continues to be readily available throughout the United States. There are reports of methamphetamine and other abused drugs being detected in aerosols, 2-6 but none that perform detection by an electrochemical sensor. The detection of drugs of abuse in aerosols is particularly interesting as a gateway to the detection in breath, which could have important implications for roadside detections and aid for overdose victims. As a proof of concept, we chose to study methamphetamine, but this system is generalizable to any redox active molecule. Electrochemical sensors are useful for field detection because they are small, simple, and cost-effective. 7-9 One limitation when employing electrochemical sensors for aerosol detection is that most electrochemical experiments need to be performed where at least two electrodes are electrically connected through

electrolyte solution. This can be accomplished by the use of a collector volume (particle into liquid sampling, PILS), which holds the electrodes.

For PILS experiments, the limitation then arises that the analyte in the aerosols is often significantly diluted before detection. Using low collector volumes can mitigate this issue. Microfluidics have been used to maintain stable, small collector droplets, but these still often require internal standards for quantitation. Previously, we demonstrated the ability to detect redox-active molecules in liquid aerosols that coalesced into 200 nL to 10  $\mu$ L droplets pipetted onto a glassy carbon surface. This technique, termed particle-into-liquid sampling for nanoliter electrochemical reactions (PILSNER) showed promise at detecting emerging environmental micropollutants in aerosols. However, due to geometric constraints of fitting two electrodes into a volume without capacitive coupling or faradaic feedback, this method was still limited to droplets with

Received: January 27, 2022 Accepted: March 23, 2022 Published: April 13, 2022





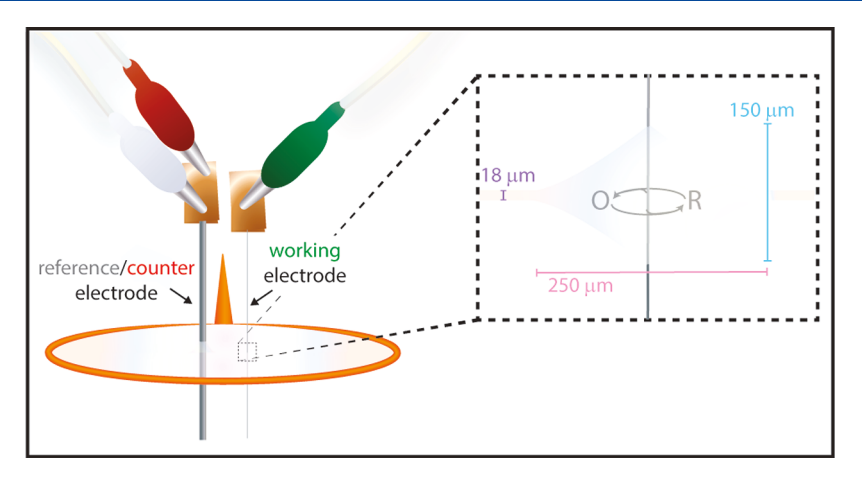


Figure 1. Schematic showing the experimental setup where the bubble wall solution contains 1 mM ferrocene methanol in 0.1 M potassium chloride (KCl) with 0.1% Triton X-100. The working electrode is a 10  $\mu$ m diameter carbon fiber, and the reference/counter electrode is a 1 mm diameter platinum wire. The inset shows the wetting of the working electrode, including the experimentally determined dimensions for the bubble wall (18  $\mu$ m) and wetting meniscus (150  $\mu$ m along the working electrode and 250  $\mu$ m along the bubble wall).

 $0.2~\mu L$  volumes. Additionally, the analytical figures of merit of PILSNER can be drastically improved by increasing the aerosol collection efficiency of the collector volumes. Collector geometries that maximize the surface area to volume ratio, like films, may be particularly useful at collecting aerosols.

Free liquid films, or bubble walls, are thin (hundreds of nm to  $\mu$ m) walls of water suspended in a solid frame and stabilized at the air interface by organized layers of surfactant molecules. In 2009, a preliminary study was presented by Caruana and coworkers describing voltammetry in a bubble wall cell. 12 In their system, a 25  $\mu$ m diameter gold wire was pushed through a surfactant film formed in the support of a loop. The film was not entirely free-standing, as the loop edge remained in contact with a bulk solution to make the connection to a counter and reference electrode. They observed a linear dependence of the peak-to-peak separation and scan rate, which they attributed to diffusion in the uniquely bounded geometry of their meniscus (or electrode wetting region). A bubble wall maximizes the surface area to volume ratio, enabling one to enhance the collection efficiency of the PILSNER technique and keep the electrodes at a distance to avoid voltametric distortion even at very low volumes.

Here, we present a thorough study of redox species in a free-standing bubble wall. In these experiments, a two-electrode configuration was employed by placing a microwire (diameter  $10-25~\mu m$ ) and 1 mm diameter platinum wire through a bubble wall. Figure 1 shows a schematic representation of the experiment with experimentally determined dimensions. A well-behaved mediator, ferrocene methanol, was dissolved into the bulk bubble solution and used for voltammetric investigations. We then applied this system to the voltammetric detection of aerosolized methamphetamine. This study offers a detailed introduction to electrochemistry in soap bubbles, proposes a useful application for the unique system, and postulates on the possibility of studying 2D diffusional processes using the proposed experimental design.

## MATERIALS AND METHODS

Chemicals and Materials. Ferrocene methanol (FcMeOH, 97%), Triton X-100, and chloroplatinic acid (8% wt in  $H_2O$ ) were purchased from Sigma-Aldrich. Hydrochloric acid (HCl) was obtained from Alfa Aesar. Potassium hydroxide

(KOH) was obtained from VWR (ACS grade). Tris-(bipyridine)ruthenium(II) chloride (Ru(bby) $_3^{2+}$ ), methamphetamine, and cocaine hydrochloride were obtained from Sigma-Aldrich. Potassium ferricyanide was obtained from Acros Organics (99+% ACS reagent). Millipore water (Millipore Milli-Q $_1$  18.20 M $\Omega$  cm $^{-1}$ ) was used to prepare solutions, and 10  $\mu$ m diameter carbon fibers obtained from Thornel (P-55 pitch-based fibers) and 10 and 25  $\mu$ m diameter platinum wires from GoodFellow were used as the working electrodes; 1 mm diameter platinum wire from GoodFellow was used as the reference/counter electrode. A commercially available bubble wand was used to form the bubble wall, and a commercially available humidifier was used to provide humid experimental conditions to prolong bubble lifetime.

Sensor Fabrication and Model Mediator Voltammetry. The bubble wall was formed by submerging a bubble wand into a weigh boat containing the 0.1 M KCl and 0.1% (v/v) Triton X-100 solution with and without 1–2 mM ferrocene methanol. The working and reference/counter (*i.e.*, pseudoreference) electrodes were pushed through the wall to form the electrochemical cell. Cyclic voltammetry was performed in a 0.1 M KCl and 0.1% Triton X-100 solution containing 1 mM ferrocene methanol using a two-electrode configuration connected to a CHI 601E potentiostat.

**Electrodeposition for Wetting Parameters.** Electrodeposition was performed by amperometry in a 0.1 M HCl and 0.1% Triton X-100 solution containing 40 mM chloroplatinic acid using a two-electrode configuration connected to a CHI 601E potentiostat. The amperometric depositions were performed at -0.8 V *versus* platinum wire and variable run times, dictated by bubble lifetime.

**Aerosol Experiments.** The bubble wall was formed by submerging a bubble wand into a weigh boat containing the 0.25 M KCl and 0.1% (v/v) Triton X-100 solution with and without 10 mM ferricyanide or methamphetamine. The working and reference/counter electrodes were pushed through the wall to form the electrochemical cell. A carbon fiber acted as the working electrode ( $d=10~\mu m$ ) and a platinum wire, as the reference/counter electrode (d=1~mm). Cyclic voltammetry was performed in a bubble wall connected to a CHI 6012D potentiostat.

As a control, a relatively well-behaved electron mediator (ferricyanide) was nebulized into a bubble wall. Similar to

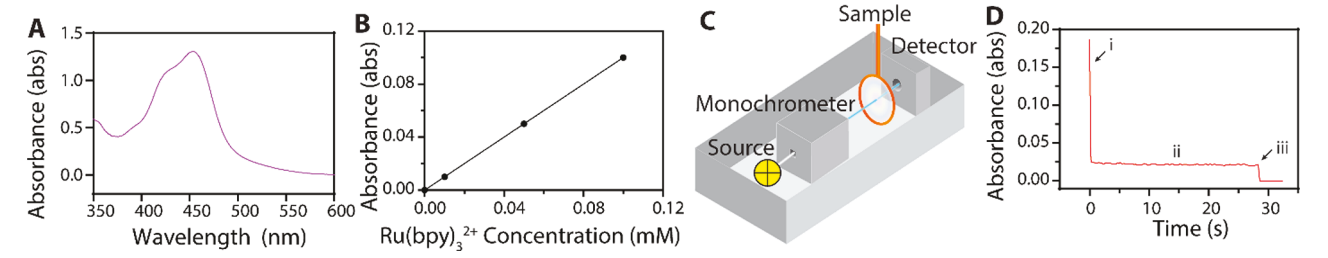


Figure 2. (A) Absorbance spectra of 0.1 mM  $\mathrm{Ru}(\mathrm{bpy})_3^{2+}$  in 0.1 M KCl with 0.1% Triton X-100 between 350 and 600 nm. (B) Absorbance *versus* concentration plot for  $\mathrm{Ru}(\mathrm{bpy})_3^{2+}$  in 0.1 M KCl with 0.1% Triton X-100 at 452 nm. The  $R^2$  value is 0.999, and the slope is 12 933  $\mathrm{M^{-1} \cdot cm^{-1}}$ . (C) Schematic representation of the UV—vis experiments for determining bubble wall thickness. The bubble wand was placed between the light source and detector. (D) Sample time course measurement of the absorbance in a bubble wall at 452 nm. The bubble wand insertion can be seen at point i; the bubble wall absorbance can be seen in the region labeled ii, and the bubble popping can be visualized at point iii. All measurements were taken using a Jasco V-650 spectrophotometer, which was blanked with a solution of 0.1 M KCl and 0.1% Triton X-100.

ferrocene methanol, ferricyanide is "well-behaved" (1 electron, fast heterogeneous kinetics, and outer sphere); however, ferricyanide is very water-soluble compared to ferrocene methanol (low millimolar solubility in water). As the aerosolized droplets have approximately femtoliter volumes, to observe a fast response from aerosol collection, we nebulized solutions with concentrations of 10 mM ( $\sim 10^4$ -10<sup>7</sup> molecules/aerosol). All aerosols were generated by an Aerogen Pro-X controller through an Aerogen Solo mesh nebulizer, which produces droplets of 1-5  $\mu$ m in diameter. The bubble wall consisted of 0.25 M KCl and 0.1% v/v Triton X-100, and the aerosol solution contained 10 mM ferricyanide in 0.25 M KCl. Cyclic voltammetry was performed from 0.5 to -0.5 V versus platinum wire and scanning at 0.5 V/s. Between all runs, the electrodes and bubble wand were cleaned with rinses of water and ethanol. Additionally, for each experiment, a full scan (0.5 V to -0.5 to 0.5 V versus platinum wire) was collected as the background before pausing the voltammetry for aerosol collection. For safety, all aerosol experiments were conducted within a fume hood. To limit noise from this environment and perturbations to the bubble wall, a Faraday cage was used and the voltammetry was paused during aerosol generation. The nebulizer was directed at the bubble wall for  $\sim$ 10 s and then turned off, and the voltammetry was resumed for subsequent scans.

The detection of methamphetamine aerosols proceeded as described above, except the bubble wall and aerosol solution were adjusted to pH 11 with KOH and the voltammetry was performed from 0 to 1.5 V *versus* platinum wire. The high pH allowed for the proton-coupled electron transfer kinetics to be more favorable, allowing for the distinction of methamphetamine oxidation from water oxidation on the carbon fiber electrode.

All aerosol experiments were performed in a Faraday cage within a fume hood.

**Microscopy.** Scanning electron microscopy (SEM) images were taken using a Helios 600 Nanolab dual beam system (FEI, Hillsboro, OR) at 10 kV and 0.34 nA. The Analyze Particles function on ImageJ (NIH, Public Domain) was used to determine nanoparticle size and coverage. A digital microscope from Park Systems was controlled by a PC for image collection and measurement software (CoolingTech).

**Spectroscopy.** Energy dispersive X-ray (EDX) spectra were obtained using a Hitachi S-4700 Cold Cathode Field Emission Scanning Electron Microscope and INCA PentaFET-x3 (Oxford, Abingdon, UK) system at 20 kV and 10  $\mu$ A. Ultraviolet—visible spectroscopy was used to determine the

film thickness. Absorption spectra for 0 to 0.1 mM Ru(bby) $_3^{2+}$  in 0.1 M KCl and 0.1% Triton X-100 were recorded between 350 and 600 nm. The peak absorbance was determined (452 nm) and graphed *versus* concentration. The resultant slope (12 933 M $^{-1}$ ·cm $^{-1}$ ) was used in subsequent calculations as the molar absorptivity coefficient ( $\varepsilon$ ). The bubble film was formed by submerging the bubble wand into a 1 mM Ru(bby) $_3^{2+}$ , 0.1 M KCl, 0.1% Triton X-100 solution. The bubble wand containing the film was placed between the light source and the cuvette holder. Time-dependent absorbance spectra were recorded at peak absorbance, and the Beer–Lambert Law was used to calculate the bubble wall thickness (path length). All spectra were obtained using a Jasco V-650 spectrophotometer blanked with a solution of 0.1 M KCl and 0.1% Triton X-100.

## ■ RESULTS AND DISCUSSION

The generation of a bubble wall and subsequent placing of microwires within the wall sets up a rather unique electrochemical cell geometry. Below, we outline several experiments that allow us to elucidate the geometry before describing the electroanalysis in the system.

We used ultraviolet-visible (UV-vis) spectroscopy to measure the bubble wall thickness. In accordance with the Beer-Lambert Law,

$$A = \varepsilon l C_{\text{dve}}$$

the absorbance (A) depends on the concentration of the dye  $(C_{\text{dye}})$ , the molar absorptivity  $(\varepsilon)$ , and the path length (l)through which light traverses from the source to the detector. We chose to probe tris(bipyridine)ruthenium(II) chloride, which exhibits a strong absorption at 452 nm. Figure 2A shows the absorption spectrum of 1 mM tris(bipyridine)ruthenium-(II) chloride in 0.1 M KCl and 0.1% Triton X-100 in a cuvette where l = 1 cm. Figure 2B shows the linear relationship between peak absorbance and tris(bipyridine)ruthenium(II) chloride concentration, yielding a molar extinction coefficient of ~13 000 M<sup>-1</sup>·cm<sup>-1</sup>. Using knowledge of the molar extinction coefficient and the dye concentration, we backed out the path length (1) when the bubble wall was placed between the source and detector (Figure 2C). Figure 2D shows a typical spectrum, where we tracked the absorbance at 452 nm with time as a bubble wall was placed in front of the detector. The initial high absorbance value corresponded to the intact bubble wall entering the light path (Figure 2Di), and the sharp step down to 0 coincided with the bubble popping (Figure 2Diii). While the light path traversed through the bubble wall, we detected a steady absorbance response (Figure

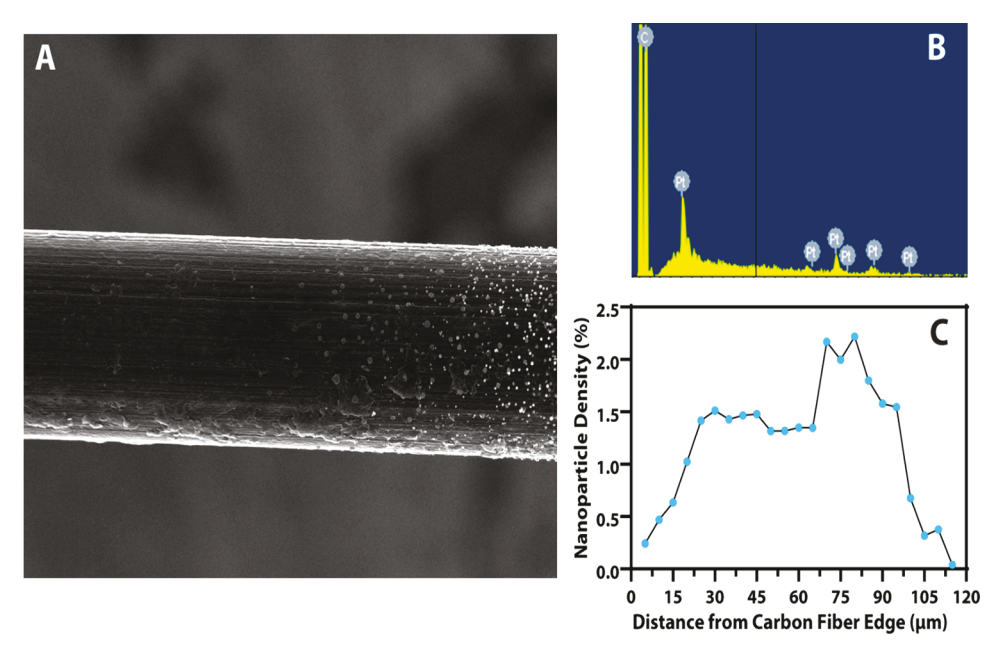


Figure 3. SEM image and corresponding EDX spectra of platinum nanoparticles ( $r = 60 \pm 19$  nm for this sample, N = 160) deposited on a carbon fiber microwire ( $r = 5 \mu m$ ). (A) Shows a transition from an area without nanoparticles to an area with nanoparticles. (B) Representative EDX spectra of platinum nanoparticles on the carbon fiber. (C) Plot of the nanoparticle density as a function of distance along the carbon fiber.

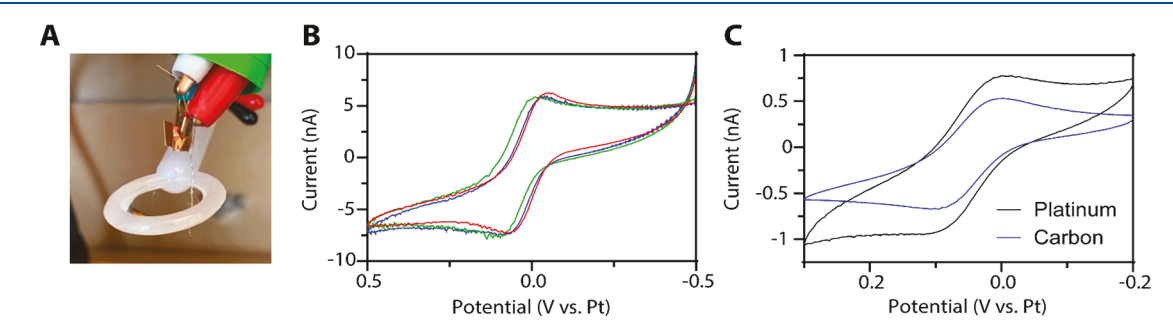


Figure 4. (A) Image of the experimental setup, where a carbon fiber  $(d = 10 \ \mu\text{m})$  and platinum wire  $(d = 1 \ \text{mm})$  were pushed through the bubble wall and operated as the working and reference/counter electrodes, respectively. (B) Cyclic voltammograms in bubble walls (N = 3) containing 2 mM ferrocene methanol and 0.1% Triton X-100 in 0.1 M KCl measured by a carbon fiber  $(d = 10 \ \mu\text{m})$  working electrode *versus* platinum wire (reference/counter) at a scan rate of 0.1 V/s. (C) Cyclic voltammograms in bubble walls composed of 1 mM ferrocene methanol and Triton X-100 in 0.1 M KCl (scan rate 0.05 V/s). The blue voltammogram was obtained on a 10  $\mu$ m diameter carbon fiber *versus* a platinum wire (reference/counter), and the black voltammogram was obtained on a 10  $\mu$ m diameter platinum wire *versus* a platinum wire (reference/counter). All voltammograms are plotted in the polarographic convention.

2Dii) that was used to calculate the bubble wall thickness as 18  $\pm$  1  $\mu$ m. We did not precisely control the placement of the bubble to ensure the incoming light would contact the same point in each bubble film because we found that the placement did not largely influence the measurement, as shown by the reported precision.

To visualize the bubble wetting dynamics with tens of nanometer resolution, we electrodeposited (see Materials and Methods above) platinum nanoparticles ( $r = 40 \pm 20$  nm, N = 345) onto the carbon fiber microwire from a bubble wall loaded with 40 mM chloroplatinate ( $H_2PtCl_6$ ), 0.1 M HCl, and 0.1% Triton X-100. Scanning electron microscopy showed a region of deposition on an otherwise bare carbon fiber. Figure 3A shows the "edge" or one transition region from bare fiber to a region with deposited nanoparticles. Energy dispersive X-ray (EDX) spectroscopy confirmed that the nanoparticles were platinum (Figure 3B). We quantified the nanoparticle density as a function of distance from an "edge" to better resolve the profile. Figure 3C shows a typical profile of nanoparticle

density as a function of distance. These analyses indicated that the bubble wets  $157 \pm 30~\mu m~(N=5)$  of the carbon fiber microwire. These observations have reasonable agreement with optical visualization from the digital microscope (Figure S1A) but offered resolution down to tens of nanometers. Images taken in plane with the bubble wall suggest that the wetting extends laterally along the film ~125  $\mu m$  from the microwire, as seen in Figure S1B. This value has reasonable agreement with complementary measurements obtained with a digital microscope (Figure S1C).

Voltammetry was performed in the bubble wall by passing a carbon fiber or platinum wire ( $10-25~\mu m$  diameter) working electrode and platinum wire (1 mm diameter) reference/counter electrode through the bubble wall, such that the effective electrode geometry was a baseless cylinder (Figure 4A). The reproducibility of the voltammetry in different bubble walls (Figure 4B) and the small relative standard deviation ( $\sim$ 5%) of the bubble wall thickness measurements (see above) indicate that the solution and effective electrode

geometry were sufficiently similar between bubbles. Slight shifts in the observed half-wave potentials were observed due to shifts in the reference potential over time at the platinum wire, which was often avoidable by a thorough cleaning or replacement of the reference wire. The parameter that provides the most significant effects on the voltammetric signal is the wetting, which dictates the effective electrode area and solution geometry at the electrode. This parameter can be modulated by the insertion of different materials to act as the working electrode. The effective electrode area can be tuned by electrode material and the relative hydrophilicity. We enhanced the oxidative peak current by 42% (N = 3) by replacing the 10  $\mu$ m carbon fiber with a 10  $\mu$ m platinum (Figure 4C). The current enhancement is the intuitive result since platinum is more hydrophilic than carbon, and thus, the bubble will wet the platinum surface more.

An exciting application of this system is for aerosol collection and electrochemical detection. The bubble wall geometry is unique in that the surface area to volume ratio is maximized. Compared to a 100 nL spherical droplet, a 100 nL bubble wall (assuming a thickness of 18  $\mu$ m) increases the surface area by 2 orders of magnitude. Additionally, spreading the volume in a thin layer allows for easy electrode placement and can avoid diffusion layer overlap, where voltammetric distortion is caused by capacitive coupling and/or faradaic feedback. Simple diffusion of electrochemical products can be considered using the Einstein equation,

$$x = \sqrt{6Dt}$$

where x is the displacement (m), D is the diffusion coefficient (m²/s), and t is the time (s). To avoid faradaic feedback of ferrocene methanol ( $D=7\times10^{-10}$  m²/s) for a 60 s measurement in a spherical droplet, one would be required to use a volume an order of magnitude higher than the bubble wall (assuming a 18  $\mu$ m thickness). This model is simplified to make the geometric argument. The contributing modes of mass transfer in the bubble (2D diffusion and convection) are not completely understood at this time but will be an area of future study.

Unlike canonical voltammetry in bulk solutions on cylindrical electrodes, we observe peaking even at very low scan rates that scales with the square root of the scan rate (Figure S4). As such, we do not attempt quantitation in this first report of an application and instead propose the application as a binary result indicating the presence of an illicit substance. The increased surface area of this electrochemical cell makes the detection solution itself an efficient aerosol collector. As a proof of concept, we aerosolized a 10 mM ferricyanide solution and used voltammetry to detect the species using wires pushed through the bubble wall (as described in the previous sections). Aerosols were generated using a mesh nebulizer, which was directed at the bubble wall for ~10 s before detection by cyclic voltammetry (Figure S4). As shown in Figure 5A, after 10 s of exposure, the characteristic voltammetry of ferricyanide could be observed with currents on the order of 20 nA.

For a more applicable detection, we demonstrate the ability to distinguish methamphetamine in liquid aerosols. Methamphetamine is among the most trafficked illicit drugs in the United States<sup>1</sup> and is most often consumed via pipe smoking. As such, methamphetamine exists in aerosols around users and manufacturing sites. On carbon electrodes, methamphetamine can undergo electrochemical oxidation in water that releases

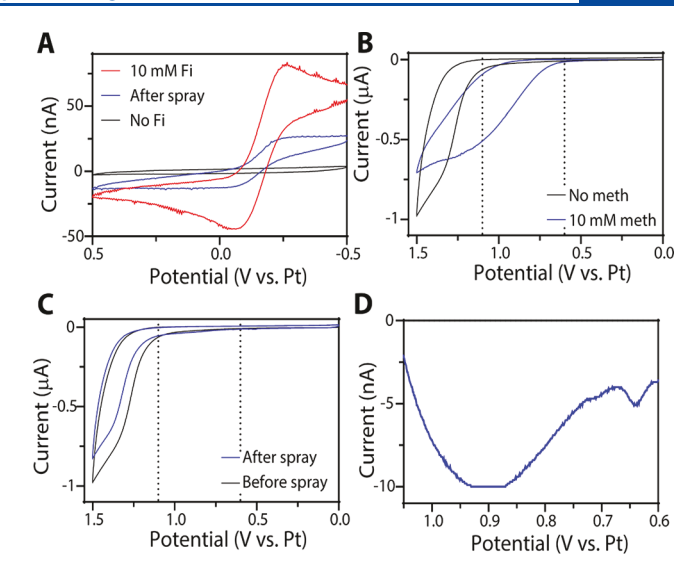


Figure 5. (A) Cyclic voltammograms in a bubble wall containing 0.25 M KCl and 0.1% Triton X-100 (black) and containing 10 mM ferricyanide (red). The blue trace is the 0.25 M KCl and 0.1% Triton X-100 bubble wall after 10 s of exposure to 10 mM ferricyanide (0.25 M KCl) aerosols. Scan rate was 0.5 V/s. (B) Cyclic voltammograms in a bubble wall containing 0.25 M KCl and 0.1% Triton X-100 (black) and containing 10 mM methamphetamine (blue). Scan rate was 0.2 V/s. (C) Cyclic voltammograms in a bubble wall containing 0.25 M KCl and 0.1% Triton X-100 (pH = 11) before (black) and after (blue) 10 s of exposure to 10 mM methamphetamine (in 0.25 M KCl, pH = 11) aerosols. Scan rate was 0.2 V/s. (D) Background subtracted voltammetry (blue - black scan from panel C) showing anodic current from collected methamphetamine aerosols. For all panels in this figure, voltammetry was performed with a 10  $\mu$ m diameter carbon fiber versus a 1 mm diameter platinum wire (reference/counter) and are plotted in the polarographic convention.

proton.<sup>13</sup> This proton-coupled process is kinetically more favorable at a high pH, and the oxidation of methamphetamine in a bubble wall at pH = 11 is shown in Figure 5B. Figure 5C shows the voltammetric detection of methamphetamine after ~10 s of exposure to 10 mM methamphetamine liquid aerosols. A background-subtracted voltammogram in Figure 5D shows nanoampere current resulting from methamphetamine oxidation. It should be noted that slight increases in capacitance likely indicate that the bubble thickness or electrode contact is increasing during collection (Figure S5). At this time, we do not know if the aerosols are integrated into the film or collected on top. If aerosol droplets do integrate, they may efficiently mix into the bubble volume where analyte becomes quickly homogeneous throughout the bubble wall or the detection may depend on the droplets landing and integrating near the working electrode.

We have observed that microliter droplets have the tendency to slide over the surfactant wall, as these surfactant molecules are arranged with the hydrophobic tails toward the surface of the bubble. Interestingly, a voltammetric response was recorded when a 5  $\mu$ L droplet containing a redox-active molecule (10 mM cocaine) was pipetted such that it visibly collided with the working electrode on top of the bubble wall but did not contact the reference/counter wire (Figure S6). As the reference/counter was only connected through the aqueous bubble wall, this observation suggests that one can "catch" aqueous droplets on an aqueous film and detect redox active contents with little to no dilution by electrochemical connection through the bubble wall. As the mass transfer to

the electrode throughout the meniscus is ambiguous and the aerosol collection/integration is not well understood, quantitation in this system is difficult. The ambiguity is exacerbated by bubble evaporation occurring on the time scale of the experiment that may be leading to convection. For this work, we managed longer experiments by humidifying the faraday cage before and throughout the measurements. In a humid environment with minimal vibrations (on a heavy/air table), the aqueous bubble reproducibly survived for tens of minutes. A more field-practical solution may be a shift to ionic liquid films. In addition to their low vapor pressure, ionic liquids may not require the use of surfactants, which could allow better integration of aerosols. In ionic liquid systems, quantitation could be simplified. In aqueous, surfactant-containing systems, the previous report<sup>12</sup> discussed interesting electrostatic effects by use of charged surfactants in a bubble wall. The electrostatic-induced migration of differently charged molecules through the film can allow for selective enhancement at or removal of a molecule from the electrode surface, presenting a potentially useful separation step to the electrochemical detection.

#### CONCLUSION

In summation, we have demonstrated a complete characterization of a bubble wall using electrochemistry. We demonstrate ultraviolet-visible spectroscopy can be used to quantify the bubble wall thickness, and electrodeposition coupled with scanning electron microscopy can be used to quantify how extensively the soap bubble wets the electrode. Not only can one perform electrochemistry in a soap bubble wall and robustly characterize the bubble's geometry, but also we demonstrate the surface area of a soap bubble wall is maximized compared to the droplet counterpart by two orders of magnitude. The thin film nature of the bubble wall allows it to act like a butterfly net to catch aerosols. When aerosols integrate with the soap solution (or contact the electrode surface), their contents can be analyzed. As a proof-of-concept, we applied this sensing modality to the detection of methamphetamine in aerosols. While the detection at this time is binary in terms of the presence of an illicit substance, the geometric characterization can give rise to robust quantitative analysis moving forward. These results set a foundation to capture and analyze aerosol contents in a unique environment, and the application to illicit substance detection in aerosols is of utmost importance to first responders.

## ASSOCIATED CONTENT

#### Supporting Information

The Supporting Information is available free of charge at https://pubs.acs.org/doi/10.1021/acs.analchem.2c00462.

Micrographs of bubble wetting, bubble volume calculations, scan rate studies, photographs of the experimental setup, capacitance changes, and additional voltammetry for aerosol detection (PDF)

## AUTHOR INFORMATION

## **Corresponding Author**

Jeffrey E. Dick – Department of Chemistry, The University of North Carolina at Chapel Hill, Chapel Hill, North Carolina 27599, United States; Lineberger Comprehensive Cancer Center, School of Medicine, The University of North Carolina at Chapel Hill, Chapel Hill, North Carolina 27599, United States; orcid.org/0000-0002-4538-9705; Email: jedick@email.unc.edu

#### **Authors**

Kathryn J. Vannoy – Department of Chemistry, The University of North Carolina at Chapel Hill, Chapel Hill, North Carolina 27599, United States; Occid.org/0000-0002-5723-9755

Nicole E. Tarolla – Department of Chemistry, The University of North Carolina at Chapel Hill, Chapel Hill, North Carolina 27599, United States; orcid.org/0000-0001-7523-9604

Philip J. Kauffmann — Department of Chemistry, The University of North Carolina at Chapel Hill, Chapel Hill, North Carolina 27599, United States

Rebecca B. Clark – Department of Chemistry, The University of North Carolina at Chapel Hill, Chapel Hill, North Carolina 27599, United States; orcid.org/0000-0002-0323-2523

Complete contact information is available at: https://pubs.acs.org/10.1021/acs.analchem.2c00462

#### **Author Contributions**

K.J.V. and J.E.D. designed all experiments and wrote the manuscript. K.J.V. performed the voltammetry experiments and took the microscopy images. K.J.V. and N.E.T. performed the deposition and scanning electron microscopy experiments. K.J.V. and P.J.K. performed the electroanalysis of the collected aerosols. J.E.D. and R.B.C. performed the UV—vis experiments. All authors approve the final version of this manuscript.

#### Notes

The authors declare no competing financial interest.

## ■ ACKNOWLEDGMENTS

This work was completed with financial support from the Chemical Measurement and Imaging Program in the National Science Foundation Division of Chemistry under Grant CHE-2003587. K.J.V. acknowledges support from the National Institute of Justice under Grant 2020-R2-CX-0036. We thank Rezvan Kazemi, Silvia Voci, Nicole Walker, Sondrica Goines, Nathan Park, and Joshua Reyes-Morales for helpful discussions. We also thank Sharon Clark for the donation of the bubble wand that started this mess.

### REFERENCES

- (1) National Drug Threat Assessment; U.S. Department of Justice, 2020; https://www.dea.gov/sites/default/files/2021-02/DIR-008-21%202020%20National%20Drug%20Threat%20Assessment\_WEB.pdf.
- (2) Krakowiak, R. I.; Poklis, J. L.; Peace, M. R. Journal of Analytical Toxicology 2019, 43 (8), 592-599.
- (3) Stephanson, N.; Sandqvist, S.; Lambert, M. S.; Beck, O. J. Chromatogr. B: Anal. Technol. Biomed. Life Sci. 2015, 985, 189–196.
- (4) Postigo, C.; Lopez de Alda, M. J.; Viana, M.; Querol, X.; Alastuey, A.; Artinano, B.; Barcelo, D. Anal. Chem. (Washington, DC, U. S.) 2009, 81 (11), 4382–4388.
- (5) Viana, M.; Querol, X.; Alastuey, A.; Postigo, C.; de Alda, M. J. L.; Barceló, D.; Artíñano, B. *Environ. Int.* **2010**, 36 (6), 527–534.
- (6) Lin, Y.-C.; Hsiao, T.-C.; Lin, A. Y.-C. Water Res. 2020, 172, 115495.
- (7) Shaw, L.; Dennany, L. Current Opinion in Electrochemistry 2017, 3 (1), 23-28.
- (8) Khorablou, Z.; Shahdost-fard, F.; Razmi, H.; Yola, M. L.; Karimi-Maleh, H. Chemosphere 2021, 278, 130393.

- (9) Rebelo, P.; Costa-Rama, E.; Seguro, I.; Pacheco, J. G.; Nouws, H. P. A.; Cordeiro, M. N. D. S.; Delerue-Matos, C. *Biosens. Bioelectron.* **2021**, *172*, 112719.
- (10) Sameenoi, Y.; Koehler, K.; Shapiro, J.; Boonsong, K.; Sun, Y.; Collett, J., Jr; Volckens, J.; Henry, C. S. J. Am. Chem. Soc. **2012**, 134 (25), 10562–10568.
- (11) Kauffmann, P. J.; Park, N. A.; Clark, R. B.; Glish, G. L.; Dick, J. E. Aerosol Electroanalysis by PILSNER: Particle-into-Liquid Sampling for Nanoliter Electrochemical Reactions. *ACS Measurement Science Au* **2021**; DOI: 10.1021/acsmeasuresciau.1c00024.
- (12) Braide-Azikiwe, D. C. B.; Holt, K. B.; Williams, D. E.; Caruana, D. J. Electrochem. Commun. **2009**, *11* (6), 1226–1229.
- (13) Švorc, L.; Vojs, M.; Michniak, P.; Marton, M.; Rievaj, M.; Bustin, D. J. Electroanal. Chem. 2014, 717-718, 34-40.

